Appl. Phys. A 72, 573–580 (2001) / Digital Object Identifier (DOI) 10.1007/s003390100761

Applied Physics A
Materials
Science & Processing

Growth mechanisms for single-wall carbon nanotubes in a laser-ablation process

C.D. Scott[1,*], **S. Arepalli**[2], **P. Nikolaev**[2], **R.E. Smalley**[3]

[1] EM2, NASA Johnson Space Center, Houston, TX 77058, USA
(E-mail: c.d.scott@jsc.nasa.gov)
[2] GB Tech/Lockheed Martin, P.O. Box 58561, Houston, TX 77058, USA
[3] Center for Nanoscience and Technology, Rice University, Houston, TX 77005, USA

Received: 2 November 2000/Accepted: 3 November 2000/Published online: 23 March 2001 –

Abstract. Mechanisms proposed in the literature are compared with a current scenario for the formation of single-wall carbon nanotubes in the laser-ablation process that is based on our spectral emission and laser-induced fluorescence measurements. It is suggested that the carbon which serves as feedstock for nanotube formation not only comes from the direct ablation of the target, but also from carbon particles suspended in the reaction zone. Fullerenes formed in the reaction zone may be photo-dissociated into C_2 and other low molecular weight species, and also may serve as feedstock for nanotube growth. Confinement of the nanotubes in the reaction zone within the laser beam allows the nanotubes to be 'purified' and annealed during the formation process by laser heating.

PACS: 42.62.Fi; 81.05.Tp; 82.80.Ch

The purpose of this paper is to investigate mechanisms of single-wall carbon nanotube (SWNT) formation in the pulsed laser-ablation process. Time- and space-dependent emission spectroscopic and laser-induced fluorescence measurements are obtained during production of SWNTs within a double-tube reactor in a 1200 °C oven. It is proposed that suspended carbon clusters accumulate in the inner tube due to repeated laser pulses. Catalyst atoms and small carbon molecules, including C_2, are generated from further laser pulses impinging on these clusters, producing additional feedstock for carbon nanotube growth. Laser ablation, in effect, reduces the amount of amorphous or graphitic carbon that contaminates the SWNTs.

Single-wall carbon nanotubes were first discovered in the soot of an arc process used for making fullerenes [1]. Arc production was improved with the use of suitable catalysts and gas media; but there has been a longstanding problem of making very pure SWNTs [2]. In the meantime, the pulsed laser-ablation process for production of single-wall carbon nanotubes was developed by Guo et al. [3, 4] and Thess et al. [5] at Rice University. Nanotubes produced by laser ablation are purer (up to about 90% pure) than those produced in the arc process. In the Rice design, nanotubes are synthesized in argon flowing in a 25-mm tube inside a 56-mm tube, all heated to 1473 K in a tube furnace. A composite ablation target is located in front of the 25-mm inner tube, and consists of 1 at. % each of Ni and Co uniformly mixed with graphite. This configuration resulted in the best purity and yield of SWNTs of the configurations tested. It was suspected that the effect of the 25-mm inner tube was somehow to confine spatially the laser-ablation plume and maintain conditions more conducive to nanotube formation and growth. A single flow tube without any inner tube has been used in some configurations. Differing concepts of laser ablation use a single pulsed laser or two pulsed lasers operating at different wavelengths; other concepts use a continuous laser [6, 7]. Various combinations of catalysts have been tried, including iron, platinum, cobalt, nickel, and yttrium. Although SWNTs were detected in a great variety of processes, it is clear that only a few concepts can produce reasonable amounts of SWNTs. Moreover, their purity is generally not very good or not reported. The major impurities in the product are amorphous carbon, graphite particles, catalysts, and fullerenes. Other impurities that have been detected include silicon and various hydrocarbons, which are probably due to impurities introduced from unknown sources, including water, and may be from the quartz reactor tube itself.

The apparatus for producing SWNTs by the laser-ablation process at NASA Johnson Space Center (JSC) closely follows the configuration of Rice University. Minor modifications were made to the design to accommodate spectroscopic diagnostic and laser-induced fluorescence (LIF) instrumentation. The details and results from these measurements have been described previously [8, 9].

The detailed mechanism and reactions leading to formation of SWNTs are still not well understood. There have been a number of proposed mechanisms published [4–6, 10–15]. All are gas-phase processes that start with a source of carbon evaporated from a surface due to heating by the laser pulses or through heating by electric arcs or solar radiative fluxes. Processes in which carbon comes from a hydrocarbon feedstock

*Corresponding author.

are not considered here. Carbon nanotube formation from evaporated carbon requires a metal catalyst such as nickel, cobalt, iron, yttrium, etc. It has been found that bimetallic catalysts are more productive than single metals. Various configurations of laser-ablation experiments have been reported. They range from the dual laser pulsed system first used at Rice University to continuous lasers used in various laboratories. Each technique has certain aspects in common and they have led to various proposed mechanisms for the formation of single-wall carbon nanotubes. The principal differences between modeled mechanisms are the time scales on which nanotubes form and the state of particles from which nanotubes are deemed to grow.

In an early proposal [4, 5], sometimes called the 'scooter' mechanism, atoms of the catalysts Ni and Co are envisioned to attach to a fullerene or a graphene sheet. The catalyst atoms prevent the closing of the fullerene as additional carbons attach and lead to the formation of tubes. A single atom or a few atoms circulate (scoot) around the open end of the tube and adsorb small molecules of carbon and convert them into a tubular graphene-like sheet. The tube grows until too many catalyst atoms aggregate on the end of the nanotube. The large particles either detach or become over-coated with sufficient carbon to poison the catalysis. This allows the tube to terminate with a fullerene-like tip or with a catalyst particle. No mention of the time scale for nanotube formation was given for this model. The 'scooter' concept probably occurs very early in the process and may be followed by a mechanism in which SWNTs grow out of catalyst particles saturated with carbon after they have had time to aggregate. Since it was found that bimetallic catalysts improved SWNT yield, it was suggested that carbon mobility increased with two catalyst metals as compared to only one [4].

Zhang et al. [10] investigated the production of SWNTs in a nitrogen atmosphere, comparing the product with that produced in argon in similar conditions. Their findings indicated that the nanotubes were created in the high-temperature zone close to the target, in a region where nitrogen was essentially excluded by the ablation products. Later, after mixing of the plume with background nitrogen, amorphous carbons were formed that had nitrogen inclusions.

A continuous-wave (CW) carbon dioxide laser was used to produce SWNTs by Maser et al. [6]. They heated a graphite rod containing Ni/Y and Ni/Co catalysts in an argon atmosphere. They found that Ni/Y (4.2/1 at. %) yielded the most nanotubes, followed by the Ni/Y (2/0.5 at. %) mixture, then Ni/Co (2/2 at. %). The Ni/Y (4.2/1 at. %) catalyst mix is the same as that found to be best in the arc method by Journet et al. [2]. Because they found that the SWNTs were deposited very close to the target, they concluded that SWNTs must be formed very rapidly in the gas phase, either in the hot plasma plume or very close to it, where the temperature is still high enough to support their growth. They suggest that the temperature of the hot region around the laser-ablation spot on the target is high enough to assure SWNT growth without an external oven. Since external gas flow rates are very low around the target, the time scale could be rather long for nanotube formation. It is interesting to note that the CW laser ablation is similar to arc ablation in that the background gas and catalyst mix found to be best is the same as in the arc process. This may imply that heat transfer and diffusion dominate continuous processes as compared with pulsed processes.

In a single pulsed Nd:YAG laser-beam experiment Yudasaka et al. [11] found that for pulses with only 0.1-s intervals (10 Hz) the nanotube production was superior to longer intervals and that the amount produced was greater. However, the size of tubes was not influenced by pulse intervals from 0.1 to 120 s. They concluded that the surface temperature that is influenced by average energy flux affects the rate of production.

Using a 20-ms-duration pulsed CO_2 laser in single-pulse mode to ablate graphite containing 0.6 at. % Co/Ni catalysts, Kokai et al. [12] investigated the effect of oven temperature on nanotube growth. They found that larger diameter nanotubes are produced at higher temperatures, which is consistent with the results of Bandow et al. [13]. Kokai et al. reported a yield greater than 60% for an oven temperature of 1473 K. Using high-speed video and emission spectroscopy, they found that carbonaceous materials with SWNTs were visible about 3 ms after the beginning of the laser pulse. Blackbody emission from clusters was observed for more than one second. They suggested that SWNTs grow from molten carbon–metal particles via supersaturation at ablation temperatures, followed by segregation at about 1593 K. This model is based on C-Ni and C-Co eutectics. A continuous supply of hot carbon clusters and the maintenance of a hot SWNT growth zone during the 20-ms laser pulse are important. They also suggest that the temperature of the SWNT growth zone may be higher than 1473 K.

Yudasaka et al. [14] examined the effect of different catalyst combinations on nanotube growth in a pulsed laser (YAG) ablation facility. They proposed a mechanism similar to that of Kokai et al. [12] in which the laser heats the surface of the target, forming molten carbon and catalysts that are ejected from the surface. As the molten particles cool, dissolved carbon segregates from the metal and SWNT growth occurs. The yield depends on the laser power and on the amount of Ni and Co in the target. Their best yield was found to obtain with Ni/Co/C in the atomic ratio of 0.15/0.15/99.7.

To investigate the possibility that fullerenes may be an efficient feedstock, Zhang and Iijima [15] irradiated a target of pressed C_{60} and Ni/Co catalyst powders within a tube furnace. They found that SWNTs are produced in low yield at 673 K, but almost none are found at room temperature. They compared this with a graphite/catalyst mix at 673 K and found almost no nanotubes. They suggest that carbon species, mainly excited atoms and small clusters, first ablate from the target and form a plasma zone. The plasma cools by expansion and mixing with ambient argon until local thermodynamic equilibrium (LTE) is established. SWNTs are formed at the stage where the plasma zone is hot and dense. The species ablated from the C_{60} and graphite targets differ due to the presence of pentagons in C_{60} and only hexagons in graphite. Di-atom production would be greater in the C_{60} case because of lower bonding energy. Thus, there would be a greater excess of thermal energy, hence a greater flux of growth species and a higher effect of catalysts that would increase the growth rate of SWNTs. Arepalli et al. [16] excited C_{60} vapor by double-pulsed lasers and found a long persisting emission of C_2 Swan bands. Because of the very short lifetime of C_2 Swan bands, this implied that excited C_2 was produced over a long period. They suggested that photo-fragmentation of C_{60} may result in production of electronically excited C_2. It

was already known that C_2 is a photo-fragmentation product of laser-excited C_{60} [17–19]. Fullerenes are products of laser ablation of graphite when no catalysts are present, and they are found with SWNTs when metal catalysts are present. Therefore, photo-fragmentation and decomposition of fullerenes and the 'shrink wrap' phenomenon (spontaneous decomposition of $C_n^* \rightarrow C_{n-1}^* + C_2$, $n \leq 58$) should produce significant amounts of C_2 to serve as feedstock for SWNT growth.

A study of the dynamics of the laser-ablation plume in an argon atmosphere was carried out by Puretzky et al. [20]. They recorded plume images at various times from 100 µs to about 3 s. Also, they probed the flow at various times and locations with LIF of Co, C, C_2, and C_3 and laser-induced luminescence (LIL) of particles. Spontaneous emission from the plume was observed at early times, which decreased until LIF/LIL dominated. Because they saw no particulates very early in time, they discounted the idea that the surface emits molten particles; favoring, instead, the idea that carbon and catalyst clusters form as the plume cools. They observed long-persisting Co by LIF, from which they inferred that catalyst clusters are slow to form ($\sim$ 2 ms at 1273 K). From these and other considerations Puretzky et al. [21] posed the model that SWNT formation occurs over a period of milliseconds to seconds in the laser-ablation oven. They moved their oven with respect to the target to shorten the residence time of ablation products in the high-temperature zone. Fewer nanotubes were then seen and they tended to be shorter.

1 Experiments

In the following, we investigate the laser-ablation process in an oven to assess a potential mechanism for nanotube growth. It is well known that laser ablation of graphite, without catalysts, produces C_{60} and other fullerenes [22]. However, as indicated by the previous discussion, the role of condensation of ablation products and the mechanisms involving the catalysts are still open to some speculation. Relatively optimal conditions were determined at Rice University by trial and error parametric studies. The best known condition for producing SWNTs is one in which argon, at about 67 kPa, flows slowly (about 3 mm/s) down a 25-mm inner tube (Fig. 1). A 12-mm-diameter graphite target, containing 1 at. % each of cobalt and nickel, is located at the end of the tube. The tube and target are enclosed in a 56-mm tube, all of which are placed in a tube furnace heated to 1473 K. Two Nd:YAG pulsed lasers are fired along the axis of the tubes to ablate the end of the target. One operates at its second harmonic, 532 nm, and the other, 50-ns later, operates at 1064 nm. The pulse energy is 0.3 J for each laser; and each laser produces a fluence of about 1.5 J/cm^2 on the target. These lasers operate at repetition rates of 10 to 60 Hz. We shall develop an understanding of SWNT production by the laser-ablation process by examining what is known and draw inferences from these facts.

The visible plume produced by the laser pulses is about 3 to 6 mm long and 6 mm in diameter [8]. The plume temperature was estimated to be 3000–4000 K based on C_2 Swan-band spectra. As the plume expands, the temperature drops and its emission decreases significantly. This plume of ablation products ('mushroom') expands away from the target and eventually forms a ring vortex that propagates upstream [20, 21].

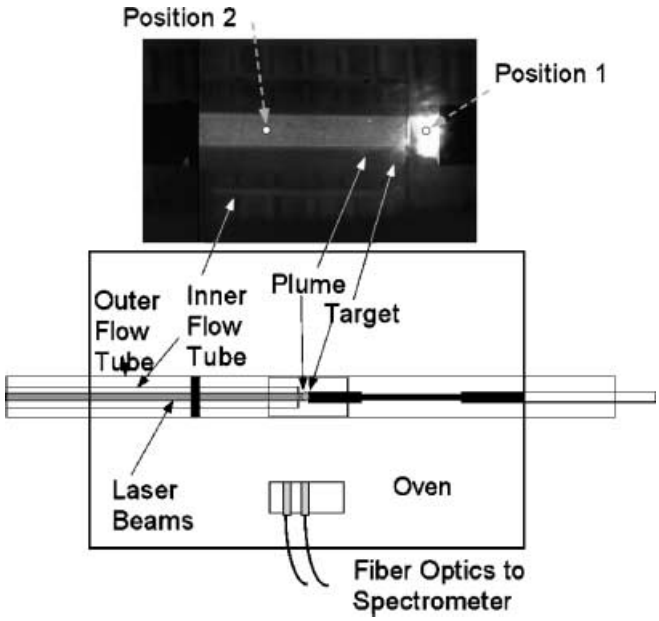

Fig. 1. Schematic of laser-ablation apparatus for production of SWNTs showing the plume and laser-induced fluorescence upstream of the target. Locations of spectral data collection are noted

The present transient intensity measurements of the plume, at several distances from the target, show that luminous ablation products propagate relatively slowly upstream. This is consistent with Puretzky et al. [20, 21] who acquired intensified charge coupled device (ICCD) camera images taken by Raleigh scattering and laser-induced luminescence of the flow in a single-pulse mode (as compared to our continuously pulsing mode). They found that a ring vortex propagates very slowly (on order of milliseconds) far upstream from the target. In our measurements with continual pulses at 10 or 60 Hz, we see that a quasi-steady-state condition develops in which ablation products containing vapors and

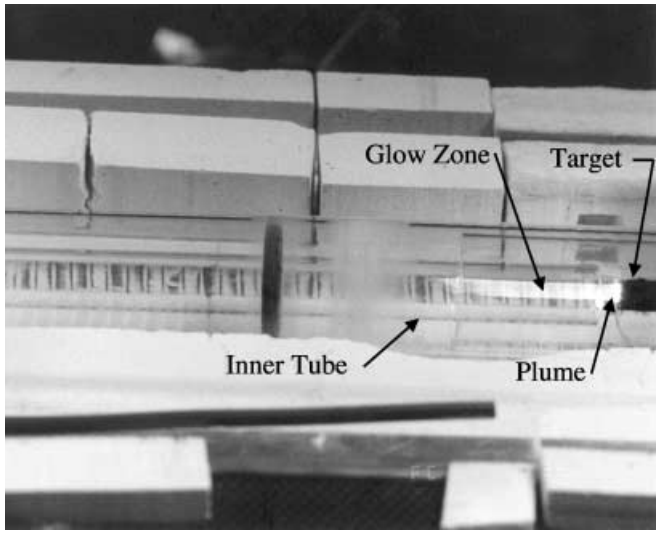

Fig. 2. Photograph of open laser-ablation oven showing laser plume and laser-induced fluorescence in the inner tube upstream of the target

condensed suspended particles propagate through the flowing argon and mix by diffusion and convection eddies. The zone upstream of the target seems to have eddy-like motion seen in the glow of laser-induced luminescence. See Fig. 2, which is a photograph of the open oven taken while the lasers are being fired. A notch filter was used to eliminate laser radiation from the exposure. It shows the target, the plume, and the glow zone. The diameter of the glow zone is about the diameter of the laser beams.

Emission spectra taken in the bright plume zone at times as early as 1 μs are mainly due to C_2 Swan-band radiation. There is also an underlying continuum. At somewhat later, but still very early times (< 2 μs), we see the appearance of C_3 near 400 nm. At much later time (greater than 50 μs), we see only blackbody emission [9]. The C_2 Swan bands persist for at least 50 μs, although the radiative lifetime of the upper state is only about 100 ns. This implies that the formation of excited C_2 must continue for at least 50 μs after the laser pulse. Exchange reactions could lead to formation of atomic carbon, which could recombine to form excited C_2, but these reactions are very fast under these conditions. We thus would expect that recombination radiation would disappear very rapidly. A model calculation that includes small carbon molecules and fullerenes indicates that the principal production of C_2 may be from C_{60} photo-dissociation. (A study of emission of C_2 Swan bands in laser-excited C_{60} vapor was reported in [16].)

Transient emissions from the plume zone (1.5 mm from the target) were obtained with a 10-nm bandpass filter centered at 510 nm (the $\Delta v = 0$ band of the C_2 Swan system). They indicate that the characteristic decay times are 1.2 μs and 95 μs, as shown in Table 1. The early-time character of decay does not seem to be related to plume propagation, which occurs over a longer time scale.

Up to roughly 1 μs after the laser pulses, the spectra in the glow zone consist of the C_2 Swan system plus a little blackbody or other continuum. This period is compared with the later period in which the C_2 Swan bands are absent, leaving only blackbody radiation that persists for many hundreds of microseconds. At a time as late as 100 μs the temperature of this blackbody radiation is about 2300 K, as determined from curve fits of the spectral intensity.

From studies of C_{60} excitation by high-power laser pulses, we see production of C_2 and smaller fullerenes [23]. Studies of C_{60} excitation with these same lasers show that excited C_2 is produced and lasts at least many tens of microseconds. Initially, the Swan bands are seen with what appears to be blackbody continuum having a characteristic temperature of about 3600 K [9]. In Fig. 3 we compare the transient response of C_2 emission from excitation of C_{60} with that from three locations. Two of the locations are in the laser-ablation glow zone, and one location is very near the target. Although the decay of C_2^* is seen in both C_{60} excitation and laser ablation, the decay in the C_{60}-excitation case is faster and exhibits two characteristic decay times. The first one, up to about 2 μs, is similar to very early decay of the laser plume at 1.5 mm from the target. The second period from about 3 μs to 20 μs shows slower decay. It is somewhat faster than the decay 14 mm from the target. However, we cannot say what species are emitting since no spectra were taken at that location. At 1.5 mm the spectra consist of blackbody continuum, with C_2 bands seen to at least 50 μs. No bands are seen at 100 μs,

Table 1. Characteristic decay times of emission for C_{60} excitation and for laser ablation for SWNT production. Unless otherwise noted the wavelength range is limited by a 510 ± 5-nm pass filter

Source conditions	Time period, μs	Decay time, μs	Apparent radiating species
Laser excitation of C_{60}	Very early 0.4–0.82	0.4 (no filter)	C_2 Swan bands and continuum
Laser excitation of C_{60}	Early 0.7–2.6	0.3	C_2 Swan bands
Laser excitation of C_{60}	Late 4–14	4.6	C_2 Swan bands
Laser ablation for SWNT production, 12 mm from target	Very early 0.5–1.0	0.4 (no filter)	C_2 Swan bands and continuum
Laser ablation for SWNT production, 12 mm from target	Early 1–4.5	1.2	C_2 Swan bands
Laser ablation for SWNT production, 12 mm from target	Mid 5–50	95	C_2 Swan bands, C_3 and continuum
Laser ablation for SWNT production, 12 mm from target	Late	Irregular	Blackbody continuum

only blackbody continuum. The spectra of C_{60} excitation are primarily C_2 radiation. At very early times, we see some blackbody continuum that disappears quickly. Laser excitation of C_{60} took place at temperatures up to 973 K; whereas, the laser-ablation measurements, which were taken while the oven was at 1473 K, could possibly account for some of the differences. In the absence of a catalyst, fullerenes are formed in the laser process; and they seem to form more favorably at 1473 K [3]. This is consistent with the maximum rate of formation of SWNTs that seems to occur at 1473 K.

The quality of production of carbon nanotubes decreases when the inner quartz tube is replaced with a larger diameter tube or when the inner tube is removed. It appears that the inner quartz tube that is placed just in front of the target is important for production of good-quality SWNTs. In SEM

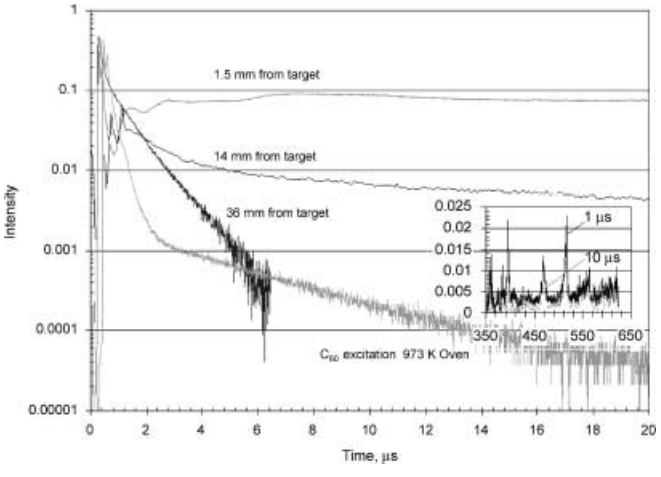

Fig. 3. Transient emission measurements 36 mm from target compared with emission due to excitation of C_{60} with a 510-nm narrow-band filter. Also shown are spectra taken at 1 and 10 μs after laser trigger in C_{60}-excitation case showing C_2 emission

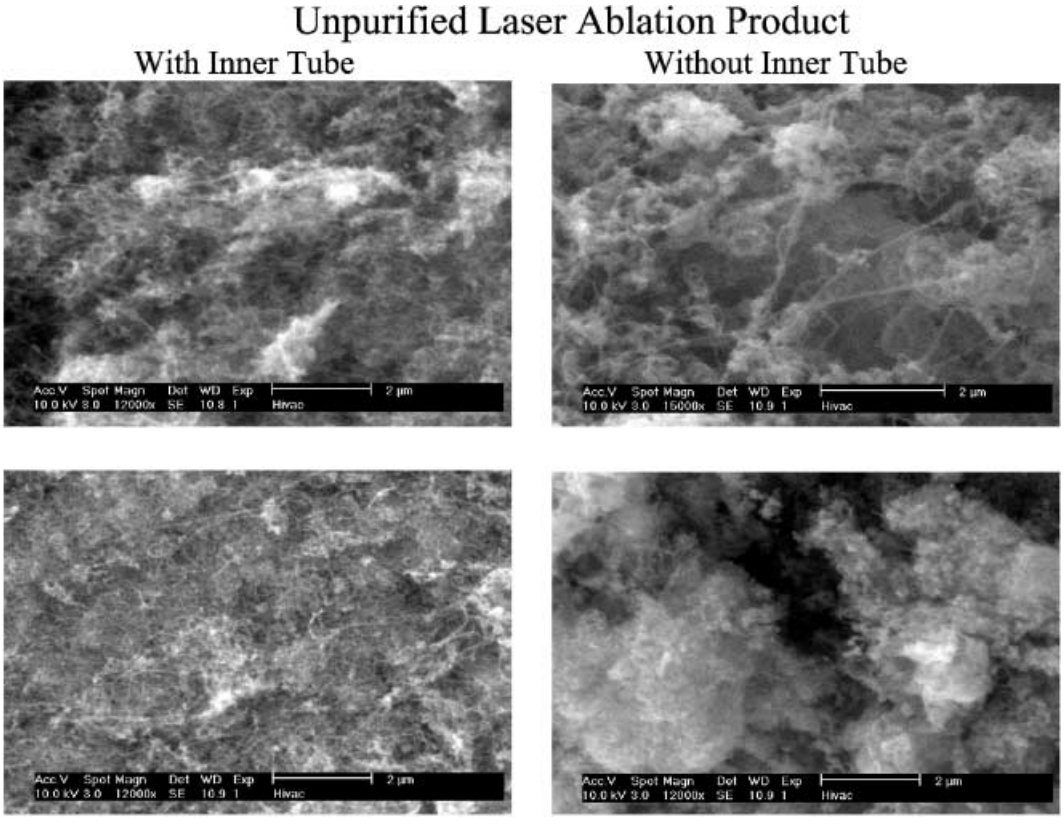

Fig. 4a,b. SEM photographs of pulsed laser-ablation product: **a** with 25-mm inner tube included and **b** with no inner tube included

images, shown in Fig. 4, we see that raw product made with the inner tube included is purer than that obtained without the inner tube.

Sequences of photographs (exposure time of 10 ns) of the laser plume emission (with the inner tube) are shown in Fig. 5. They are superimposed on the intensity history measured by a photo-multiplier (PM). The small circle on these photographs represents the zone observed by the PM, 1.5 mm from the target. Also shown are spectra taken at about the same time after the laser trigger pulse. The temperatures noted in Fig. 5 are estimated from the blackbody background spectra. The photographs correlate the development of an ablation plume with simultaneous spectra that indicate which species are radiating. The first two spectra were made with a 50-ns gate width. It is apparent that at the earliest time (about 500 ns after the trigger, or 350 ns after the laser pulse), we see significant photons from the 532-nm laser plus significant continuum that appears to be blackbody and possibly C_3 bands. We can also see some evidence of C_2. The corresponding ICCD images were taken with a notch filter that is virtually opaque to 532-nm light, thus eliminating scattered laser light. Early emission upstream of the target represents a region that glows with laser-induced luminescence. Since the plume has not reached the observation point before about 5 μs, we interpret this as being emission from particles and gases remaining from the previous laser pulses. Figure 6 presents emission histories with and without a narrow bandpass filter along with spectra obtained at various times. These measurements are obtained at a distance 33 mm upstream of the target. We have no ICCD images for this distance. Immediately after the laser pulses C_2 Swan bands and high-temperature blackbody emission appear. The C_2 Swan bands quickly disappear within a few microseconds; and the blackbody emission relaxes to near oven temperature within about 5 μs. These data indicate that particulates (carbon particles, SWNTs, and possibly fullerenes) are suspended in the upstream argon flow and are heated to a very high temperature by the laser pulses.

2 Discussion

Based on information discussed above we have formulated the following scenario for SWNT production in a laser-ablation facility. The lasers ablate the target, which produces a vapor plume of C_3, C_2, C, Ni, Co, and possibly small clusters of catalysts. No particles were seen in laser scattering experiments by Puretzky et al. This suggests that particles do not sputter from the surface as suggested by Yudasaka et al., but form later by condensation as proposed by others [3, 4]. One should note that in Yudasaka's experiment the sample was a new surface for each pulse, which was achieved by rotating the target during the diagnostic data collection [24]. This may give rise to a different plume for each new laser pulse. In our measurements, the target is fixed and we wait for about 1000 pulses to establish a steady-state condition before we start collecting any spectral data.

The 50-ns delay between the two pulses seems to enhance production. It is speculated that the delay allows the initial partially ionized plume to expand sufficiently to allow penetration by the second pulse, but before the target surface has had a chance to cool appreciably. The amount vaporized from the surface is strongly dependent on surface

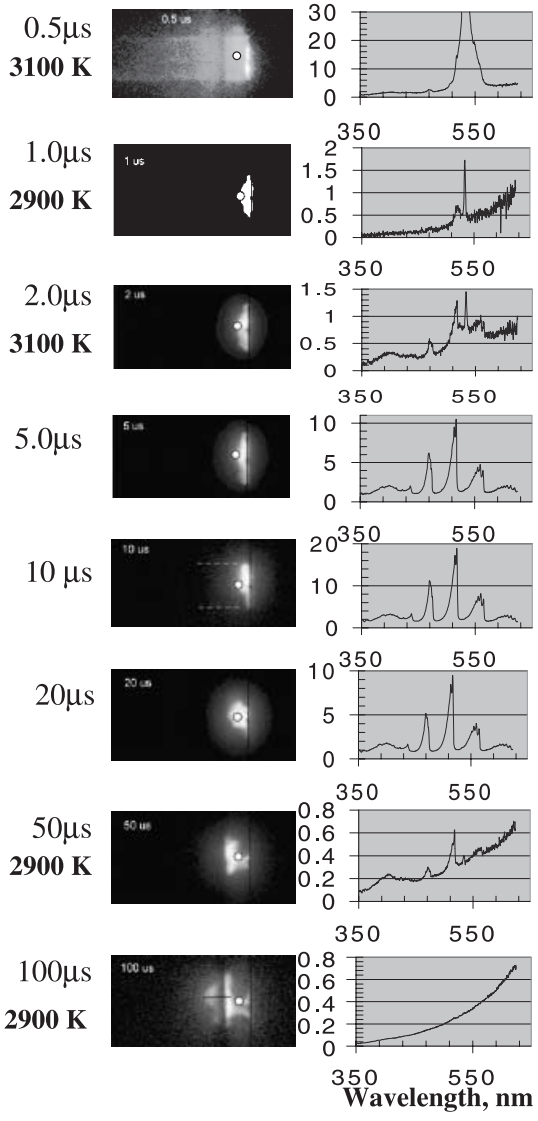

Fig. 5. Composite of spectra taken 1.5 mm from target with ICCD images. Temperatures shown are from blackbody estimates

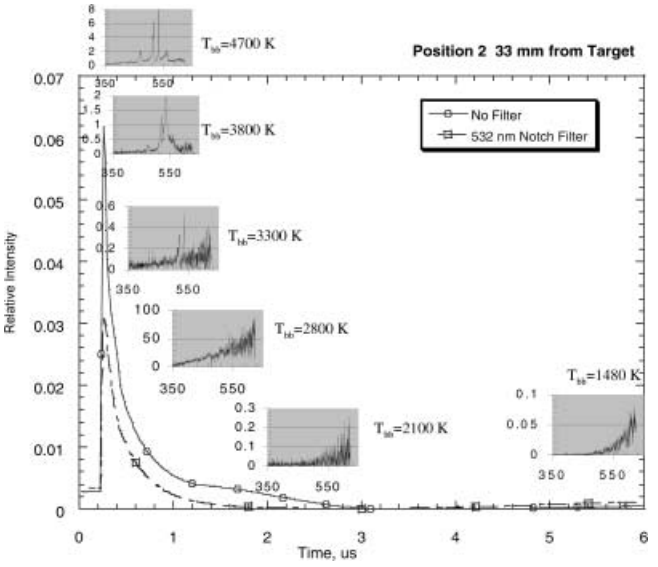

Fig. 6. Composite of transient emission measurements and spectra taken inside the inner tube 33 mm upstream of the target

temperature. After the vapor leaves the surface, small molecular weight carbon species coalesce very quickly to form larger molecules, and eventually fullerenes, including C_{60}. According to estimates of reaction kinetics, catalyst metal atoms also coalesce to form clusters, but at a much lower rate. We have measured Ni LIF to about 2.3 ms, at 1 mm and 2 mm from the target. These measurements indicate that the atom density builds up and peaks at about 100–200 µs, then decays slowly in a bi-exponential fashion, see Fig. 7. This peak LIF signal occurs after the 'mushroom head' of the plume passes this location when the blackbody temperature is about 2200 K. The peak in the emission from the plume occurs at about 60 µs. Puretzky et al. measured cobalt LIF up to about 2 ms within their moving plume [20, 21]. Our present results show decaying LIF signals at fixed locations having characteristic decay times τ of about 570 µs and 1160 µs during the periods of 300–1000 µs and 1500–6000 µs, respectively. The decay is probably due to condensation of atoms into Ni clusters, as well as expansion and dilution. We do not know which of these is dominant.

The decay seems to follow a first-order reaction scheme as evidenced by its exponential decay. Nanometer-sized catalyst particles absorb and/or adsorb low molecular weight carbon molecules, especially C_2. They may also attach to fullerenes or graphene sheets and prevent closure. As they remain open at the attachment point of particles or atoms of Ni/Co, they begin to grow into a nanotube from the carbon dissolved in or adsorbed on the catalyst. Under steady-state operating conditions at 60 Hz the average density of carbon atoms is roughly 10^{18} cm^{-3}. Most of these atoms will be found bound in molecular clusters. Thus, the actual number density of carbon particles is much smaller. These higher molecular weight species will naturally have a slower mean thermal speed than C or C_2. From calculations of the flux of carbon on catalyst particles, we can estimate the maximum possible growth rate of tubes. At an assumed minimum temperature of 1473 K, and a C-atom density of 10^{18} cm^{-3}, a (10, 10)-carbon nanotube would grow at a maximum rate of about 100 µm/µs, if the catalyst particle were one nanometer in diameter. (At a density of 10^{21} cm^{-3}, as suggested by Smalley [22], the growth rate would be three orders of magnitude greater, or 100 mm/µs.) Carbon atoms and small molecules attach to each other and form higher molecular weight carbon chains and possibly sheets of graphene. Therefore, the mass flux of carbon will be smaller due to the lower mean thermal speed. However, since the velocity depends on the inverse of the square root of the particle mass, we would expect that this would reduce the flux only by perhaps an order of magnitude relative to C_2. Then nanotubes would still grow on the order of 1 to 10 µm/µs. Isolated individual SWNTs were produced in short (0.5 s) bursts of laser pulses and deposited on silica witness plates [25]. Measurements by atomic force microscopy (AFM) indicate that the length of nanotubes is tens of micrometers long; and they grow at a rate in excess of 0.15 µm/µs. Thus, we would expect that they grow during the early time period of the plume evolution, unless the rate is severely limited by other steps, e.g. diffusion in or on the catalyst, probabilities of reaction (steric factor), absorption, etc. Ultimately, the growth may be stopped by saturation of cat-

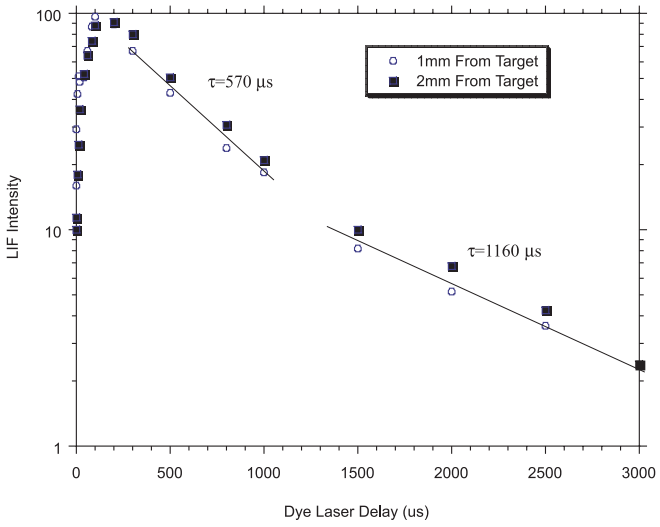

Fig. 7. Laser-induced fluorescence of nickel at distances of 1 mm and 2 mm from the target

alyst particles by an overcoat of carbon. Puretzky et al. [21] suggest that the nanotube growth period lasts on the order of seconds. Their conclusion is based on observation of long persistence of cobalt atoms (and by inference, nickel), and incomplete conversion of carbon to SWNTs at the upstream end of their reactor. This is plausible only if the SWNT-formation rate is much smaller that the rate based on kinetic fluxes of carbon on catalyst particles. Since metal particles many times larger than nanotube ropes are seen in the product, we expect that growth is limited when the large-diameter catalyst particles get poisoned or possibly break away from the nanotubes that are forming, thus terminating their growth. It is also possible that a catalyst particle has to be in the liquid form to effectively absorb incoming feedstock and channel carbon to the growing nanotube by diffusion. Since the melt temperature of very small clusters is suppressed compared to bulk material, the particle would remain liquid until its size increases sufficiently, then solidify and stop nanotube growth. Similar considerations may explain why binary metal mixtures are the best catalysts – their melting points are further suppressed.

We envision that suspended carbon clusters, particularly nanotubes, amorphous or graphitic carbon, and fullerenes build up in the 25-mm quartz tube due to repeated laser shots at 10 to 60 Hz. Laser excitation of any vapor-phase fullerenes would result in fullerene dissociation and production of C_2. Laser ablation (vaporization) of particles suspended in argon also generates C_2, other small carbon molecules, and possibly catalyst atoms. These free catalyst atoms may then re-condense into small clusters on which small carbon molecules feed the growth of nanotubes. This process is enhanced by the 25-mm tube that confines the vapor and particles in and around the laser beams so that graphitic/amorphous clusters may be re-vaporized to provide new feedstock. Some of the amorphous/graphitic carbon that adheres to nanotubes and catalyst particles may be 'cleaned off' by heating due to further laser pulses before the nanotubes drift downstream of the target in the slow argon flow. Annealing of imperfect nanotubes can occur in the high-temperature (1473 K) oven. Finally, nanotubes and other products of ablation ultimately condense on the cooler downstream region of the 50-mm tube.

A number of studies, such as [10], investigated the effect of the background gas on nanotube production. It was found that argon and nitrogen gave similar results, but helium was found to yield poorer results. This suggests that thermal conductivity and, possibly, the speed of wave expansion plays a role in nanotube formation. Since these effects are dominant in the plume-expansion region and not in the area where the ablation products have cooled to the ambient oven temperature, we expect that nanotube formation is dominant near the target and in the vicinity of laser-irradiated particles in the flow tube. The effect of the oven is to maintain a base temperature such that there is greater target ablation, slower cooling of particles, and a higher vapor pressure of small carbon and catalyst clusters. Cooling of particles is mainly from evaporation at these conditions. Therefore, diffusion through the background gas would dominate the cooling process. Thus, particles would cool more slowly in a heavy molecular weight gas, such as argon or nitrogen.

3 Conclusions

We now summarize our proposed mechanism for growth of single-wall carbon nanotubes by the pulsed laser-ablation technique. Laser pulses heat the target surface containing graphite and finely divided nickel and cobalt and vaporize them. A very hot vapor plume is formed that expands and cools rapidly. As the vaporized species cool, small carbon molecules and atoms quickly condense to form larger clusters, including possibly fullerenes. The catalysts also begin to condense, but more slowly at first, and attach to carbon clusters and prevent their closing into cage structures. Catalysts may also open cage structures when they attach to them. From these initial clusters, tubular molecules grow into single-wall carbon nanotubes until the catalyst particles become too large, or until conditions have cooled sufficiently that carbon no longer can diffuse through or on the catalyst particles. It is also possible that the particles become so coated with a carbon layer that they no longer can absorb more and nanotube growth ceases.

By comparing the spectral emission of excited species in laser ablation of a composite graphite target with that of laser-irradiated C_{60} vapor, we see some striking, but not exact similarities. This leads us to suspect that fullerenes are produced by laser ablation of catalyst-filled graphite, as is the case when no catalysts are included in the target. However, subsequent laser pulses excite fullerenes to emit C_2 that adsorbs on catalyst particles and feeds SWNT growth. However, there is insufficient evidence to conclude this with certainty since the time scale for decay of C_2 Swan-band emission differs in the C_{60}-excitation experiments, compared with the present laser-ablation measurements. Repeated laser pulses vaporize some of the confined amorphous/graphitic carbon and possibly catalyst particles. Laser pulses excite any fullerenes, which then decompose, leading to additional feedstock for SWNT growth. Because improved production and purity are observed when a 25-mm-diameter 'inner' tube is placed upstream of the target, we believe that the tube confines ablation products to the neighborhood of the

laser beam. Without the confining inner tube, ablation products, consisting of graphitic carbon clusters and catalyst particles, escape from the influence of the laser pulse and its heating.

It may be possible to improve production and purity by reversing the flow of argon, thus maintaining the ablation products exposed to the laser beams longer and vaporizing more of the amorphous carbon and large catalyst particles. This would allow them to reform as nanotubes and reduce impurities. Smaller diameter inner flow tubes that would confine the ablation products totally within the laser beams may also improve the product.

Acknowledgements. The authors thank Dr. Gary De Boer of Le Tourmeau University for analyzing the nickel LIF measurements and for useful discussions.

References

1. S. Iijima, T. Ichihashi: Nature **363**, 603 (1993)
2. C. Journet, W.K. Maser, P. Bernier, A. Loiseau, M. Lamy de la Chapelle, S. Lefrant, P. Deniard, R. Lee, J.E. Fischer: Nature **388**, 756 (1997)
3. T. Guo, P. Nikolaev, A.G. Rinzler, D. Tománek, D.T. Colbert, R.E. Smalley: J. Phys. Chem. **99**, 10694 (1995)
4. T. Guo, P. Nikolaev, A. Thess, D.T. Colbert, R.E. Smalley: Chem. Phys. Lett. **243**, 49 (1995)
5. A. Thess, R. Lee, P. Nikolaev, H. Dai, P. Petit, J. Robert, C. Xu, Y.H. Lee, S.G. Kim, A.G. Rinzler, D.T. Colbert, G.E. Scuseria, D. Tománek, J.E. Fischer, R.E. Smalley: Science **273**, 483 (1996)
6. W.K. Maser, E. Muñoz, A.M. Benito, M.T. Martínez, G.F. de la Fuente, Y. Maniette, E. Anglaret, J.-L. Sauvajol: Chem. Phys. Lett. **292**, 587 (1998)
7. M. Yudasaka, F. Kokai, K. Takahashi, R. Yamada, N. Sensui, T. Ichihashi, S. Iijima: J. Phys. Chem. B **103**, 3576 (1999)
8. S. Arepalli, C.D. Scott: Chem. Phys. Lett. **302**, 139 (1999)
9. S. Arepalli, P. Nikolaev, W. Holmes, C.D. Scott: Appl. Phys. A **70**, 125 (2000)
10. Y. Zhang, H. Gu, S. Iijima: Appl. Phys. Lett. **73**, 3827 (1998)
11. M. Yudasaka, T. Ichihashi, T. Komatsu, S. Iijima: Chem. Phys. Lett. **299**, 91 (1999)
12. F. Kokai, K. Takahashi, M. Yudasaka, R. Yamada, T. Ichihashi, S. Iijima: J. Phys. Chem. B **103**, 4346 (1999)
13. S. Bandow, S. Asaka, Y. Saito, A.M. Rao, L. Grigorian, E. Richter, P.C. Eklund: Phys. Rev. Lett. **80**, 3779 (1998)
14. M. Yudasaka, R. Yamada, N. Sensui, T. Wilkins, T. Ichihashi, S. Iijima: J. Phys. Chem. B **103**, 6224 (1999)
15. Y. Zhang, S. Iijima: Appl. Phys. Lett. **75**, 3087 (1999)
16. S. Arepalli, C.D. Scott, P. Nikolaev, R.E. Smalley: Chem. Phys. Lett. **320**, 26 (2000)
17. S.C. OBrien, J.R. Heath, Y. Liu, R.F. Curl, R.E. Smalley: J. Chem. Phys. **88**, 220 (1988)
18. D.M. Gruen, S. Liu, A.R. Krauss, X. Pan: J. Appl. Phys. **75**, 1758 (1994)
19. P. Wurz, K.R. Lykke: J. Phys. Chem. **96**, 10129 (1992)
20. A.A. Puretzky, D.B. Geohegan, X. Fan, S.J. Pennycook: Appl. Phys. A **70**, 153 (2000)
21. A.A. Puretzki, D.B. Geohegan, X. Fan, S.J. Pennycook: Appl. Phys. Lett. **76**, 182 (2000)
22. R.E. Smalley: Acc. Chem. Res. **25**, 98 (1992)
23. S.C. O′Brien, J.R. Heath, R.F. Curl, R.E. Smalley: J. Chem. Phys. **88**, 220 (1988)
24. F. Kokai: private communication
25. S. Arepalli, P. Nikolaev: Appl. Phys. Lett. **78**, 1610 (2001)